JOURNAL OF MATERIALS SCIENCE 26 (1991) 5467–5472

Photoelectron spectroscopy on metal–polymer interfaces: Ag/polybutene (Ag/PB–1) and epitaxial Sn/polybutene (Sn/PB–1)

M. JUNG, U. BASTON, P. STEINER
Fachbereich Physik, Universität des Saarlandes, D-6600 Saarbrücken, FRG
J. PETERMANN
Arbeitsbereich Kunststoffe/Verbundwerkstoffe, Technische Universität Hamburg-Harburg, Harburger Schloßstr. 20, D-2100 Hamburg 90, FRG

The interaction of metals with polymer surfaces is studied by photoelectron spectroscopy for the case of Ag/polybutene (Ag/PB–1) and Sn/polybutene (Sn/PB–1). While Ag/PB–1 shows the normal behaviour as observed for small particles, e.g., Ag/graphite; Sn/polybutene (Sn/PB–1), which grows epitaxially, shows, in addition, a component at very low coverage, which can be attributed to a Sn–O–C bond at the Sn/PB–1 interface.

1. Introduction

The transfer of crystallographic informations across an interface as one material crystallizes onto another can result in preferred orientation relationships between the atoms or molecules of both substances (epitaxy). This phenomena has been observed for a long time for various kinds of materials, but it was only shown recently, that the evaporation of some metals onto surfaces of uniaxially oriented thermoplastic semicrystalline polymers result in an oriented overgrowth of the metals [1, 2]. It was demonstrated that the classical criteria for epitaxial growth [3, 4] do not fit to the polymer–metal interfaces. The interest in these interfaces has increased recently due to electronic micro-packaging problems, in which polyimides in contact to some metals play important roles. Surface sensitive methods (XPS) indicate that metallo-organic compounds can form at these interfaces [5].

It is the purpose of this paper to compare the electronic states of metal islands (Sn, Ag) on surfaces of uniaxially oriented polybutene-1, on which one of the metals (Sn) forms an epitaxial orientation relationship with the polymer and the other does not.

2. Experimental procedure

The polymer used as a substrate was polybutene-1, PB–1 (Vestolen BT, Chemische Werke Hüls, Marl, FRG). Ultra thin films were prepared according to the method of Petermann and Gohil [6]: an 0.4% solution of the polymer in *o*-xylene was poured on a heated glass plate ($T = 150\,^{\circ}C$) where the solvent evaporated. The remaining thin polymer film was picked up with a motor driven take-up roll with a velocity of $10\,cm\,s^{-1}$. The resulting stretched film exhibits a needle crystalline morphology and a fibre texture (Fig. 1). The single film has a thickness of approximately 50 nm, and was used without further preparation for transmission electron microscopy (TEM) investigations. The TEM used was a Philips 400 T operated at 100 kV.

The photoemission experiments were performed in two different XPS spectrometers: (i) an HP 5900 ESCA and (ii) a VG ESCALAB MKII. For the experiments, dense PB–1 films were prepared in the usual way [6] on Cu-plate substrates with a film thickness of about 50–100 nm. The HP 5900 ESCA spectrometer, equipped with monochromatic AlK_{α} radiation and a charge neutralizer (flood gun) was mainly used to study the pure PB–1 films. No radiation damage of the films could be detected by photoemission in agreement with other XPS experiments [7] on pure hydrocarbon bonds. The only changes which have been detected were, a small change in the position of the C–1s line with slightly enhanced sample temperature up to 150 °C which were completely reversible with temperature cycling. This is interpreted as arising from a change in static charging of the sample after photoemission due to a change in the electrical conductivity. A detailed discussion of these results is presented elsewhere [8].

Ag and Sn films on PB–1 were investigated with MgK_{α} radiation (not monochromatic) in the ESCALAB MKII, which allows high count rates to collect reasonable statistical accuracy of the spectra especially at low metal coverage. The vacuum in the spectrometer during the measurements stayed below 5×10^{-8} Pa. The XPS spectra of the pure PB–1 films showed no significant contamination of the surfaces by oxygen. The metal overlayers were *in situ* evaporated from a directly heated W filament in the preparation chamber of the instrument. During evaporation the vacuum increased up to about 10^{-6} Pa. The sample was then introduced into the analytical cham-

0022–2461/91 $03.00 + .12

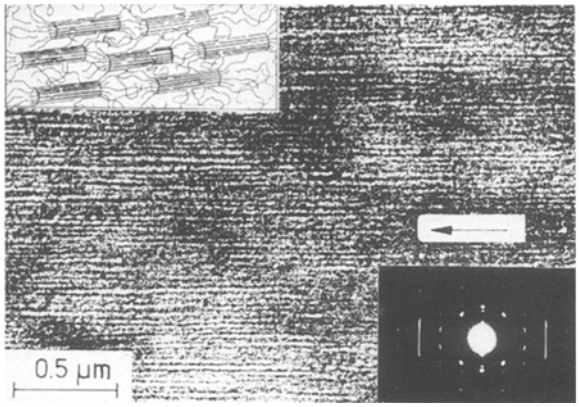

Figure 1 TEM micrograph of a PB–1 substrate film. Inserted are an electron diffraction pattern and a schematic sketch of the morphology, the arrow indicates the molecular direction.

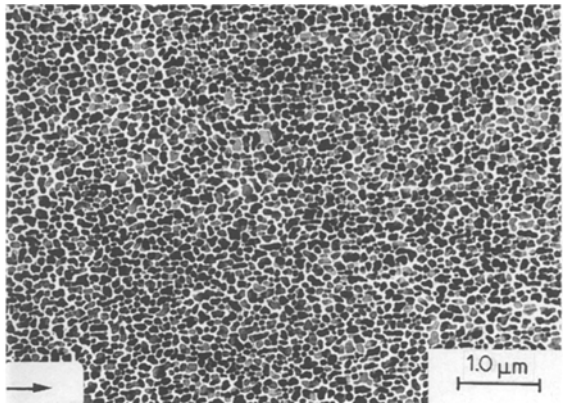

Figure 3 TEM micrograph of Sn clusters on a PB–1 substrate, the arrow indicates the molecular direction of the substrate.

ber of the instrument without braking the vacuum. The metal coverage of the films, later given in average monolayer equivalents of the metal, was determined by (i) the decrease of the C–1s signal of the PB–1 substrate and (ii) the increase of the metal signal.

3. Results and discussion

3.1. TEM Microscopy

In Fig. 2a and b electron diffraction patterns of Sn on an amorphous carbon substrate and on a PB–1 film are shown, respectively. While on the carbon substrate the diffraction of the Sn crystals results in Debye–Scherrer rings, a very well pronounced, preferred orientation is seen on the PB–1 substrate. The orientation relationship is that the polymer chain axes ([0 0 1] direction) in the *pseudo*-hexagonal unit cell of the PB–1 is parallel to the [1 0 0] lattice direction of the tetragonal Sn unit cell, but contact planes of the Sn deposit can be all ($h\,k\,0$) planes (fibre texture). On the other hand, the electron diffraction patterns of Ag on the carbon and polymer substrate do not differ and exhibit Debye–Scherrer rings. Fig. 3 presents a TEM micrograph of the Sn islands on the PB–1 film. The Sn forms islands, which coalesce to a continuous film with increasing particle size. The same morphology is true for Ag on the PB–1 films.

3.2. Photoemission

Before we discuss our XPS results for Ag and Sn on PB–1, a few general remarks about photoemission of small metal particles and islands on poorly conducting substrates are necessary. These experiments, especially metal particles on carbon, have been discussed extensively in the past [9–11] to detect the influence of the particle size on the electronic structure of the metal particles.

Two effects, especially, can contribute to core level binding energy shifts as function of the particle size, namely (i) initial state effects, due to changes in chemical bonding within the metal clusters or due to interactions with the substrates and (ii) final state effects, which arise from the interaction of the photohole, created in the photoemission process, with the electrons of the surroundings. For noble metals and sp band metals like Sn the latter effect was shown to be dominant [12, 13], and as will be shown later in the

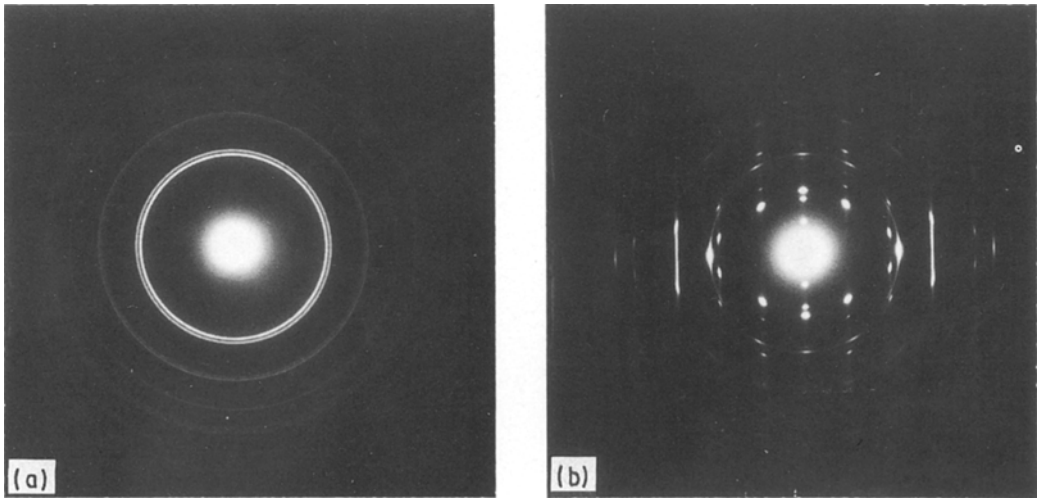

Figure 2 (a) Electron diffraction pattern of Sn crystals, evaporated on an amorphous carbon film, (b) electron diffraction pattern of Sn on a PB–1 substrate.

discussion, also dominates the results of Ag on PB–1 and Sn on PB–1. This contribution leads to core level binding energy shifts of all metal lines of the order of 1 eV, including the position of the Fermi-edge, to higher binding energies with decreasing particle size. The explanation of this behaviour is as follows: For substrates with a poorly conducting contact (weak interface interactions) to the metal cluster, the positive charge created during photoemission (one electron hole state) in the cluster cannot be screened quickly enough by electrons from the substrate (the time scale of photoemission is of the order of 10^{-15} s). The electrostatic self-energy of this charge leads to positive binding energy shifts of about $q^2/2R$, where $q \approx e$ is the positive charge remaining in the metal cluster and R the cluster radius [13]. On the other hand when the screening time is even longer than the time between two succeeding photoemission events we get an additional positive shift by a *quasi* static charging of the sample. This latter shift can be discriminated against the first by two observations: (i) The charging shift increases with increasing photon flux. Since the sampling depth in photoemission is only of the order of a few nanometres the core level lines in the substrate surfaces (in our case the C–1s line of PB–1) are shifted by the same amount and therefore the shifts of the metal cluster core level lines can be corrected against this static charging by using the substrate core level line as an energy reference (in our case it is E_B (C_{1s}) = 285.0 eV). (ii) A further distinction can be obtained if Auger lines from the metal cluster are measured in the same experimental set-up. In an Auger process the static sample charging shifts the Auger lines by the same value to lower kinetic energies as the core level lines to higher binding energies. So again this shift is removed from the data, when a substrate line is used as an internal binding energy reference. In the Auger process the initial state is a one hole state, e.g., excited as in our case by photoemission, while the final state is a two hole state with $q \approx 2e$. Therefore the Auger shifts should be about a factor 3 larger than the core level binding energy shifts, measured on the same particles, where the exact value of this factor depends, of course, on the detail of the screening response of the surrounding electrons. This has been observed for Ag and Sn on carbon [14, 15].

To discriminate between these final state effects and to observe possible differences between the interaction at the interface of Sn clusters on PB–1 and Ag clusters on PB–1 we compare their XPS and X-ray excited Auger spectra.

As mentioned earlier, in the following the C–1s signal of the substrate with a value of $E_B(C_{1s})$ = 285.0 eV is used as an internal energy calibration. Fig. 4a shows the Ag–3d core level spectra of Ag clusters on PB–1 for different cluster sizes as given by their average coverage in terms of metal monolayers. The binding energy increases with decreasing cluster size, that is, with decreasing coverage and saturates at very small coverage at a shift of 0.6–0.7 eV (see also Fig. 5) At the same time the line broadens significantly. A similar shift is observed for the position of the Fermi edge of the Ag-clusters. The Ag Auger $M_{4,5}$ VV lines for different coverages are shown in Fig. 6, given

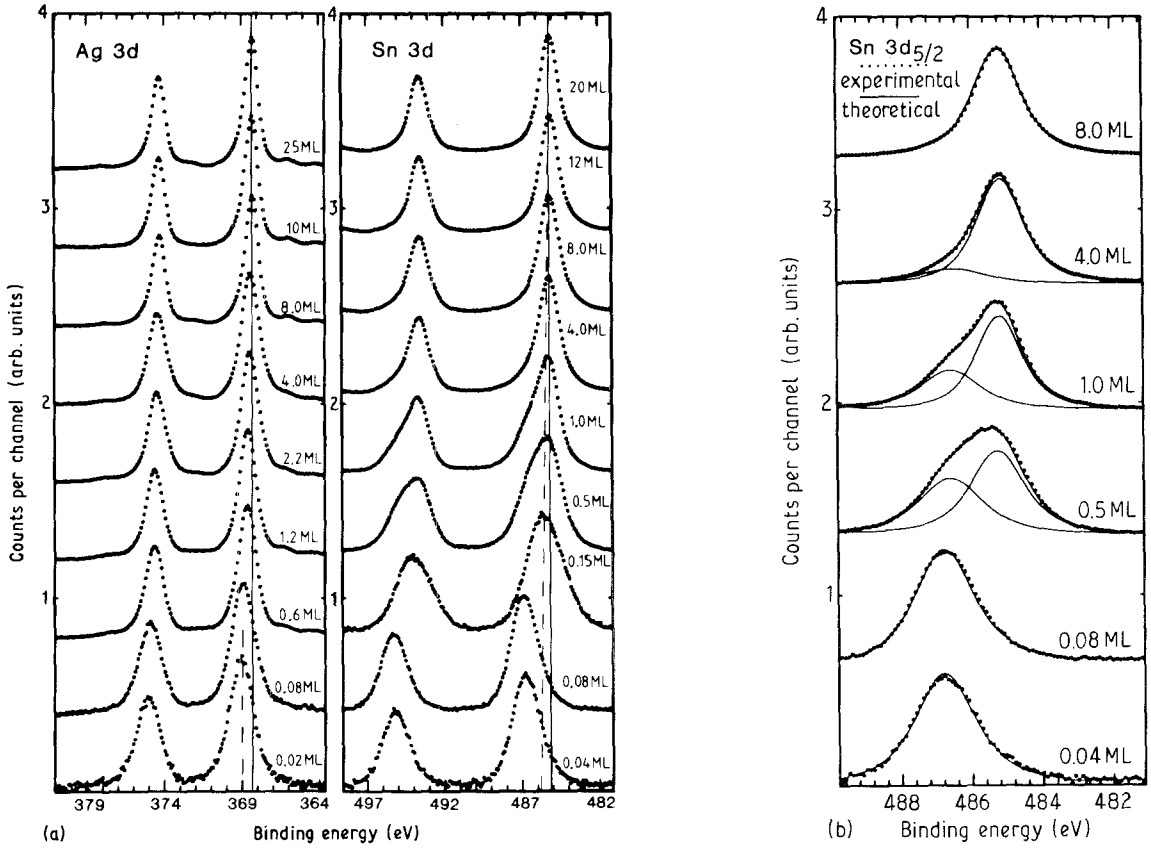

Figure 4 (a) Ag–3d and Sn–3d core level spectra of Ag clusters on PB–1 for different average Ag coverage (given in monolayers of the metal), (b) line shape analysis of the Sn–$3d_{5/2}$ line of Sn clusters on PB–1.

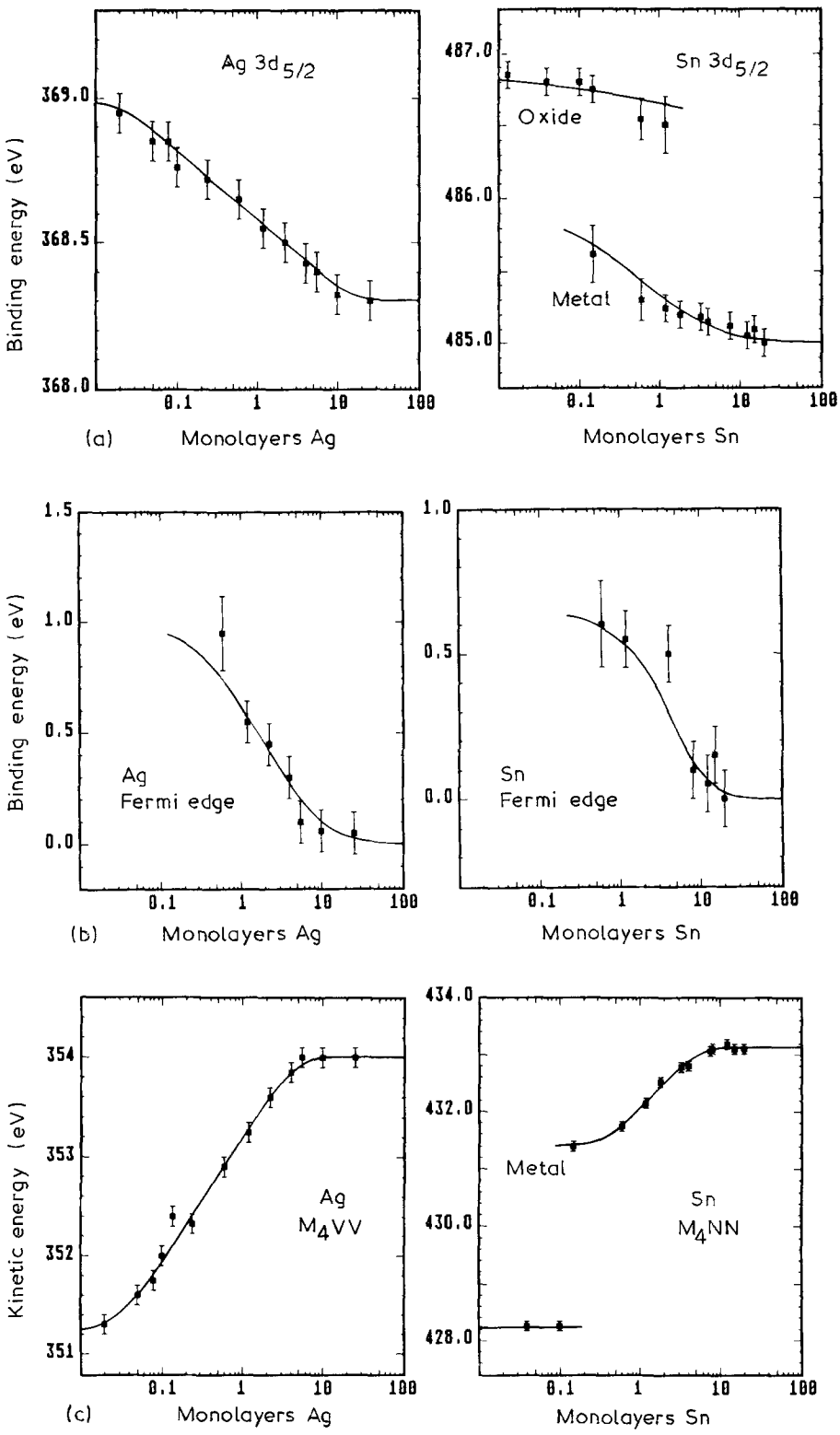

Figure 5 Binding energy and Auger energy shifts for Ag and Sn clusters on PB–1 as function of their average coverage. (a) $3d_{5/2}$ core levels shifts, (b) Fermi edge shifts, (c) Auger M_4 VV and M_4NN shifts.

on an apparent binding energy scale (the Auger kinetic energy scale in the usual way is $E_{Kin} = 1253.6 - E_B$). The shifts to higher energies are now considerably larger. The details of these shifts and structural changes in the Ag–4d valence bond levels, which are involved in these Auger transitions are discussed elsewhere [15]. As seen in Fig. 5 this shift saturates at a value of 7 eV at low coverage, which is about a factor of 3 larger than the corresponding core level shifts. These findings, as summarized in Fig. 5, leads us to conclude, that Ag clusters on PB–1 show similar photoemission spectra as Ag on carbon [10]. The intrinsic line shifts can be solely explained as arising from the dynamic self energy shift $q^2/2R$ as discussed above. There is no indication of an additional interface interaction between the Ag cluster and the PB–1 substrate.

The corresponding photoemission and Auger spectra for Sn on PB–1 are shown in Figs 4 and 6. Again we observe a shift to higher binding energies at low coverage but now the shifts at lower coverage are much larger than in the case of Ag/PB–1 (indicated by the broken line). A closer inspection of the Sn–3d line shape shows (Fig. 4c) that the Sn–3d spectra at a coverage below one monolayer are very well reproduced by a superposition of two lines where the

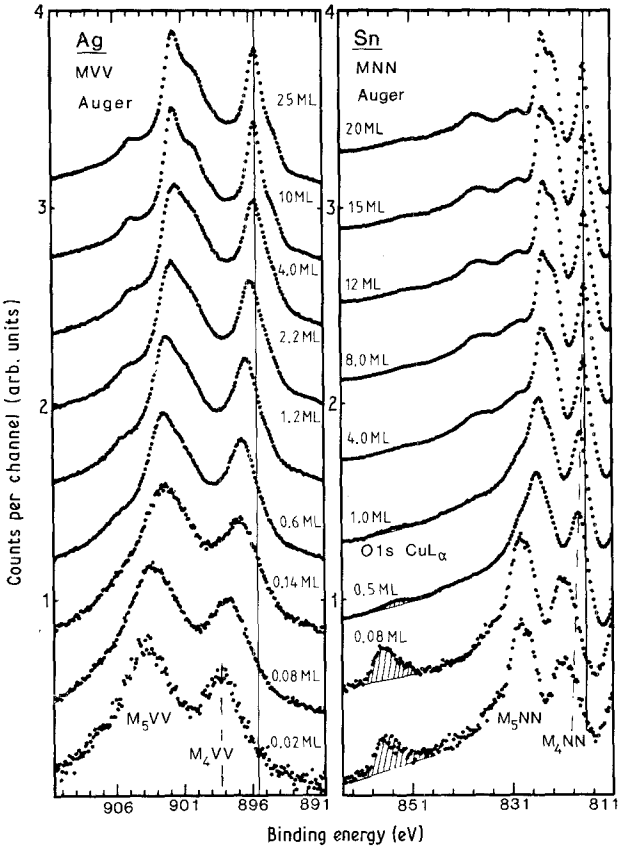

Figure 6 Ag–$M_{4,5}$ VV and Sn–$M_{4,5}$NN Auger lines of Ag clusters on PB–1 for different coverage.

relative contribution of the line at the higher binding energy, which we attribute, as will be discussed shortly, to a Sn oxide like phase at the Sn/PB–1 interface, shows a nearly coverage independent position at 486.7 eV (Fig. 5). It disappears at about one monolayer. The metallic like component at the lower binding energy shows a shift from 485.0 eV at high coverage to 485.6 eV at low coverage, very similar to the behaviour of Ag/PB–1. The large shift of 1.8 eV of the high energy component against the bulk value is typical for Sn oxides [16]. Due to the very low count rates, the shift of the Sn cluster Fermi edge could not be followed to a coverage below one monolayer but down to this point (Fig. 5) the shift is again around 0.6 eV as expected from the Ag/PB–1 data. The Sn–MNN–Auger lines are also shown in Fig. 6. Again we see the larger shifts as compared to Ag at low coverage. From this large difference we again conclude that at very low coverage a non-metallic like component appears at the Sn/PB–1 interface. In addition there appears at low coverage a signal at 855 eV. This is interpreted as an excitation of the O–1s level by parasitic CuL_α radiation from the X-ray anode material. Its energy is 323.9 eV smaller than the main MgK_α energy at 1253.6 eV. Additional experiments around 531 eV (the normal position of the O–1s line for excitation with MgK_α radiation) confirmed this interpretation. Such an O–1s signal could not be detected at the uncovered clean PB–1 film. Its intensity strongly correlated to the high energy Sn–3d component at low coverage and disappears again at higher coverage. A similar oxide like Sn feature has been observed for Sn clusters on graphite [15] at low coverage but it was completely absent for Sn films on Ni prepared under similar experimental conditions. These findings as summarized in Fig. 5 lead to the following conclusions for the interface formation of the Sn/PB–1 interface. At average coverages above one monolayer the photoemission features are very similar as for Ag/PB–1 with binding energy shifts which can be explained by the electrostatic self-energy contribution of small charged clusters, produced by the excitation process. At lower coverage there is a strong tendency towards the formation of Sn oxide like structures. From similar observations for Sn on graphite but not on Ni we conclude that during the interface formation of Sn on carbon containing substrates there is a strong tendency for the formation of Sn–O–C bonds, a not unreasonable result, since Sn is known to build easily metallo–organic compounds. From pure Sn it is well known that at low O_2 partial pressure the oxidation of Sn proceeds very slowly [17]. Therefore the presence of the C-containing surface seems to stimulate this oxidation, or the sticking coefficient of SnO-like species on these polymer surfaces is much stronger than for SnO on pure Sn. Whether this special interface with metallo–organic like bonding are the reason that islands with preferred orientation are observed for Sn/PB–1 and similar metals Te, Bi [2] which are known to build metallo–organic compounds, has to be clarified by further investigations.

Acknowledgements

The support of the "Volkswagen Foundation" and "Fonds der Chemischen Industrie" are gratefully acknowledged. This work was supported also by the "Deutsche Forschungsgemeinschaft".

References

1. J. M. SCHULTZ and S. K. PENEVA, *J. Polym. Sci., Polym. Phys. Ed.* **25** (1987) 185.
2. J. PETERMANN and G. BROZA, *J. Mater. Sci.* **22** (1987) 1108.
3. L. ROYER, *Bull. Soc. Fr. Miner. Cryst.* **51** (1928) 7.
4. G. I. FINCH and A. G. QUARELL, *Proc. Phys. Soc.* **46** (1934) 148.
5. P. S. HO, J. W. HAHN, J. W. BARTHA, G. W. RUBLOFF, F. K. LE GOUES and B. D. SILVERMAN, *J. Vac. Sci. Technol.* **A3** (1985) 739.
6. J. PETERMANN and R. M. GOHIL, *J. Mater. Sci.* **14** (1979) 2260.
7. S. AKHTER, K. ALLAN, D. BUCHANAN, J. A. COOK, A. CAMPION and J. M. WHITE, *Appl. Surf. Sci.* **35** (1988–1989) 241.
8. M. JUNG, Diplomarbeit, Universität des Saarlandes (1989).
9. M. G. MASON, *Phys. Rev.* **B27** (1983) 748.
10. G. K. WERTHEIM, S. B. DI CENZO and S. E. YOUNGQUIST, *Phys. Rev. Lett.* **51** (1983) 2310.
11. T. T. P. CHEUNG, *Surf. Sci.* **194** (1984) 151.
12. G. K. WERTHEIM, S. B. DI LENZO, D. N. E. BUCHANAN and P. A. BENNETT, *Solid State Commun.* **53** (1985) 377.
13. G. K. WERTHEIM, S. B. DI LENZO and D. N. E. BUCHANAN, *Phys. Rev.* **B 33** (1986) 5384.
14. P. STEINER, U. BASTON, M. JUNG, I. SANDER and

B. SIEGWART, in Proceedings of the German Physical Society (VI), **22** (1987) 0–104.
15. U. BASTON, Diplomarbeit, Universität des Saarlandes (1989).
16. C. D. WAGNER, in "Practical Surface Analysis", App. 4, edited by D. Briggs and M. P. Seah (Wiley, New York, 1983).
17. L. GMELIN, in "Handbuch der organischen Chemie "Zinn" Teil B" (Springer Verlag, Berlin 1971) 8 Auflage.

Received 1 December 1989
and accepted 16 May 1990